Published in final edited form as:
Chem Commun (Camb). 2013 May 4; 49(34): 3582–3584. doi:10.1039/c3cc00241a.

Molecular Insights into the Reversible Formation of Tau Protein Fibrils

Yin Luo[a], **Paul Dinkel**[b], **Xiang Yu**[c], **Martin Margittai**[b], **Jie Zheng**[c], **Ruth Nussinov**[d,e], **Guanghong Wei**[a], and **Buyong Ma**[d]

Martin Margittai: martin.margittai@du.edu; Jie Zheng: zhengj@uakron.edu; Ruth Nussinov: ruthnu@helix.nih.gov; Guanghong Wei: ghwei@fudan.edu.cn; Buyong Ma: mabuyong@mail.nih.gov

[a]Department of Physics, Fudan University, Shanghai, P.R. China

[b]Department of Chemistry & Biochemistry, University of Denver, Denver, Colorado 80208

[c]Department of Chemical & Biomolecular Engineering, the University of Akron, Akron, Ohio 44325

[d]Basic Science Program, SAIC-Frederick, Inc. CCRNP, Frederick National Lab, Frederick, Maryland 21702

[e]Sackler Inst. of Molecular Medicine. Tel Aviv University, Tel Aviv 69978, Israel

Abstract

We computationally and experimentally showed that tau protein fibrils can be formed at high temperature. When cooled, the fibrils dissociate back to monomers. Heparin promotes tau fibril formation and prevents its reversion. Our results revealed the physicochemical mechanism of reversible formation of tau fibrils.

Functional amyloids can be used in biofilms and in engineering nanomaterials; while pathological amyloids can cause neurodegenerative disorders[1]. Tau proteins may have four or three microtubule binding repeats, with both repeat forms found in the fibrils of Alzheimer's patients' brain[2]. The shortened tau proteins containing only the three repeats (K19) and four repeats (K18) have been widely used in studies of tau protein aggregation, since the remaining regions only form a disordered fuzzy coat[3]. The tau fibril may be a particularly good candidate for nanomaterials since its Young's modulus is higher than that of Aβ42 and α-Synuclein fibrils[4]. The formation of tau fibrils requires high salt concentration or the addition of negatively charged cofactors such as heparin[5], which suggests an important role of electrostatic interactions in inducing aggregation-favored conformations. However, the overall driving forces that control tau aggregation are still unclear. Here, we computationally and experimentally investigate the tau fibril formation mechanism.

Replica Exchange Molecular Dynamics (REMD) simulations were performed to study the conformational ensembles of K18 and K19 monomers. At 310 K, the distribution of secondary structures (Figure 1) in both K18 and K19 was found to be similar to the results from NMR characterization[6]. Overall, both K18 and K19 monomers are disordered in solution. The regions with relatively higher β-sheet propensity have peaks around residues 275-280, 298-311, and 330-340. Our results are very close to those obtained by NMR

Correspondence to: Guanghong Wei, ghwei@fudan.edu.cn; Buyong Ma, mabuyong@mail.nih.gov.

†Electronic Supplementary Information (ESI) available: [Supplementary Information includes the Computational and Experimental details, six figures, and one Table]. See DOI: 10.1039/b000000x/

conformational sampling, which observed that high β-sheet propensities are located in the regions spanning residues (256-261), (275-282), (307-313) and (338-346) for K18[6b]. K19 has higher β-strand propensities. Further examination revealed that the contact between the R1 and R3 repeats might promote the β-strand propensities in K19 (Sup-Figure 1, Sup-Table 1), while the R1-R3 contact in K18 was not favored due to the presence of R2. The β-strand propensities in the R1C and R3C regions increased substantially in K19; however, K18 and K19 still have qualitatively similar secondary structure distributions. The dependence of the β-strand propensities on the intra-molecular contact could change the temperature dependence of the secondary structure propensity. As shown in Figure 1B, both K18 and K19 shrunk from 310 K to 340 K, consistent with small angle X-ray scattering experiments of K19 and full length htau40[7]. The β-strand propensities of K18 and K19 increase with the compactness, which peaked around 340 K and 330 K for K18 and K19, respectively (Figure 1C). However, when the temperature is higher than 340 K, the exposed surface areas for both K18 and K19 increase and the β-strand propensities decrease quickly.

We then studied the temperature dependence of amyloid formation of K18 and K19 by simulating tau octamers. For both K18 and K19 oligomers, we observed an increase in the β-sheet propensities with an increase in temperature. Even though the initial simulation setup favored high β-sheet propensities at lower temperature, the trend reversed at the end of the simulation (Figure 2A). All the fibril-like conformers shifted to higher temperature, indicating that amyloid fibrils will be stable at higher temperature while random monomers will be favored at lower temperature (Figure 2B and 2C). The transition temperature for tau amyloid formation was found to be around 340 K, where the curves of random and β-conformation cross and the intermediate state has the highest population (Figures 2B and 2C). Since the monomers also undergo structural transition around 340 K (Figures 1B and 1C), the temperature-dependent transition of tau amyloid formation could be coupled to its temperature-sensitive monomeric properties. In order to further reveal the driving force of the temperature-dependent β-sheet propensities, we computed the nonbonded interaction energies among the tau proteins and their solvation energies. Consistent with an amyloid transition temperature at 340 K, the nonbonded interactions among the tau proteins increase sharply around 340 K (Figure 2D). Further partition of the non-bonded interactions revealed the parallel contribution of the electrostatic and van der Waals (VDW) interactions (Figures 2E and 2F), partially reflecting the favorable hydrophobic and electrostatic interactions toward fibril formation at higher temperature.

The solvation energy of the tau proteins also presents strong temperature dependence (Sup-Fig 2). Generally, amyloid fibrils have low solvation energy, which leads to their precipitation[8]. Consistently, decreased solvation and protein-solvent interactions with rising temperature were observed for K18 and K19 octamers (Sup-Fig 2A and 2B). Since the tau protein octamers adopt more compact forms at higher temperature, their smaller exclusion volumes require less energy to create a cavity in bulk solution (Sup-Fig 2C). On the contrary, the less compact random conformations adopted at lower temperature are attributed to the protein-solvent interactions (Sup-Fig 2B), which are mostly contributed by the electrostatic interactions (Sup-Fig 2D and 2E). Overall, our REMD simulations predict that tau proteins could form amyloid fibrils at higher temperature, and the tau amyloid fibrils may cold dissociate around room temperature.

We then experimentally examined the temperature dependence of tau amyloid formation using a polar sensitive fluorescence assay[9]. As expected, amyloid fibrils appeared quickly in the K18 solution with heparin (within min). Amyloid fibrils appeared slowly in the K18 solution without heparin (within hr) (Figure 3A,B). We noticed that fibrils formed in the absence of heparin appeared to disintegrate when mounted onto the grids (Fig 3B, right panels). We reasoned that this property could have originated from the temperature shift as

the filaments cooled during the mounting procedure. To test the temperature effects on tau fibril integrity we monitored changes in the emission spectra. The acrylodan fluorescence blue-shifted during amyloid formation for K18 with and without heparin (Figures 3C and 3D). After heating, the K18 solution was cooled to 275 K. There was no change in amyloid morphology in fibrils formed with heparin, and the acrylodan fluorescence blue-shifted a little further (Figure 3C), indicating further maturation of fibrils. However, the K18 amyloid fibrils without heparin disappeared after cooling to 275 K, and the main peak of acrylodan fluorescence red shifted back to the original monomeric position (Figure 3D). Meanwhile, the shoulder region between 400 – 450 nm increased, indicating an increase of soluble oligomers. Interestingly, similar results were obtained at elevated salt concentration (Sup-Fig 3). Together, the experiments confirm our computational predictions that K18 can form fibrils without heparin at elevated temperature, and that K18 fibrils cold dissociate when cooled.

K19 is not able to aggregate efficiently in the absence of cofactor, despite multiple attempts (Sup-Fig 4). The observation that K19 is kinetically more difficult to aggregate than K18 is consistent with a previous report[10] and our current computational simulations. The aggregation rates of K18 and K19 depend on the nucleation process. In amyloid formation, early ordered oligomers are usually nucleated from β-structure-rich conformations rather than from random coils[8b]. Thus, the nucleation process should correlate with the stability and the concentration of oligomers with intermediate β-strand structure. Therefore, we can use the intermediate β-strand structure propensity of K19 to compare with experimental observations of polymerization reactions of K19 at various temperatures. The K18 monomer has the highest β-strand propensity at 340 K (Figure 1C, black line), the temperature at which the intermediate β-strand structure in the K18 oligomer has the highest probability (Figure 2B, blue line). However, the K19 monomer has the highest β-strand propensity at 330 K (Figure 1C, red line), which is the lowest point for the K19 oligomer with intermediate β-strand structure (Figure 2C, blue line). Therefore, K18 can form intermediate β-strand structure more easily, facilitating the nucleation process, unlike K19.

The above results demonstrated for the first time that tau fibrils aggregate at elevated temperatures and dissociate upon cooling. This behavior is reminiscent of the cold dissociation of α-synuclein fibrils[11]. While α-synuclein fibrils dissociate at 258 K, the temperature for cold dissociation of tau fibrils is shifted to above freezing point, indicating that tau fibrils are more temperature sensitive. The cold dissociation of tau and α-synuclein fibrils raises the question of whether temperature-dependent aggregation is common for other intrinsically disordered proteins, which are characterized by a low content of hydrophobic residues and sensitivity to hydration. The hydrophobic effect is important for protein folding and cold denaturation[12]. The mechanism of cold dissociation of amyloid fibrils is more complicated, and the relative importance of hydrophobic and electrostatic interactions contributing to the cold denaturation of α-synuclein fibrils was not clear[11]. Our current study revealed parallel contributions of electrostatic and hydrophobic interactions, with electrostatic effects being more important. The molecular structure of water around proteins and solvent-induced forces have both hydrophobic and hydrophilic effects[12]. Indeed, the transition temperature for tau amyloid formation at 340 K is close to the so-called percolation transition temperature of liquid water[13]. We also computed the percolation transition temperature of hydration water around the K18 octamer and confirmed a water structure transition around 330 K – 340 K (Sup-Fig 5).

Electrostatic interactions are of fundamental importance to the reversible formation of tau fibrils. The binding of highly negatively charged heparin to tau fibrils averts cold dissociation. Interestingly, elevated salt concentrations prevented heparin-mediated fibril

growth (Sup-Fig. 6) underscoring the potential relevance of such interactions for fibril propagation in neurogenerative disorders.

In conclusion, our computational and experimental studies revealed that the formation of tau fibrils at 343 K can be reversed at around 275 K. Heparin locks the tau fibril and prevents its reversion. The temperature-dependent stabilization of the fibril is coupled to its temperature-sensitive monomeric properties, driven by both hydrophobic and electrostatic interactions. Our findings provide molecular insights into the stability of amyloid fibrils which are expected to be important for the design of new stimuli-responsive amyloid-based nanomaterials.

Supplementary Material

Refer to Web version on PubMed Central for supplementary material.

Acknowledgments

This work was supported by NIH contract number HHSN261200800001E and R01NS076619; NSF grants (CAREER Award CBET-0952624 and CBET-1158447); NSF of China (Grant No. 11074047) and RFDPHE of China (RFDP-20100071110006).

Notes and references

1. (a) Lasagna-Reeves CA, Castillo-Carranza DL, Sengupta U, Clos AL, Jackson GR, Kayed R. Molecular neurodegeneration. 2011; 6:39. [PubMed: 21645391] (b) Hardy JA, Higgins GA. Science. 1992; 256:184–185. [PubMed: 1566067] (c) Romero D, Aguilar C, Losick R, Kolter R. Proc Natl Acad Sci U S A. 2010; 107:2230–2234. [PubMed: 20080671] Knowles, dTP.; Buehler, MJ. Nature nanotechnology. 2011; 6:469–479.
2. Goedert M, Spillantini MG, Cairns NJ, Crowther RA. Neuron. 1992; 8:159–168. [PubMed: 1530909]
3. Wischik CM, Novak M, Edwards PC, Klug A, Tichelaar W, Crowther RA. Proc Natl Acad Sci U S A. 1988; 85:4884–4888. [PubMed: 2455299]
4. Adamcik J, Lara C, Usov I, Jeong JS, Ruggeri FS, Dietler G, Lashuel HA, Hamley IW, Mezzenga R. Nanoscale. 2012; 4:4426–4429. [PubMed: 22688679]
5. (a) Goedert M, Jakes R, Spillantini MG, Hasegawa M, Smith MJ, Crowther RA. Nature. 1996; 383:550–553. [PubMed: 8849730] (b) Crowther RA, Olesen OF, Smith MJ, Jakes R, Goedert M. FEBS letters. 1994; 337:135–138. [PubMed: 8287967]
6. (a) Mukrasch MD, Biernat J, von Bergen M, Griesinger C, Mandelkow E, Zweckstetter M. J Biol Chem. 2005; 280:24978–24986. [PubMed: 15855160] (b) Ozenne V, Schneider R, Yao MX, Huang JR, Salmon L, Zweckstetter M, Jensen MR, Blackledge M. Journal of the American Chemical Society. 2012; 134:15138–15148. [PubMed: 22901047]
7. (a) Shkumatov AV, Chinnathambi S, Mandelkow E, Svergun DI. Proteins. 2011; 79:2122–2131. [PubMed: 21560166] (b) Ciasca G, Campi G, Battisti A, Rea G, Rodio M, Papi M, Pernot P, Tenenbaum A, Bianconi A. Langmuir. 2012; 28:13405–13410. [PubMed: 22891813]
8. (a) Matthes D, Gapsys V, de Groot BL. J Mol Biol. 2012; 421:390–416. [PubMed: 22326493] (b) Grabenauer M, Wu C, Soto P, Shea JE, Bowers MT. Journal of the American Chemical Society. 2010; 132:532–539. [PubMed: 20020713]
9. Dinkel PD, Siddiqua A, Huynh H, Shah M, Margittai M. Biochemistry. 2011; 50:4330–4336. [PubMed: 21510682]
10. Jeganathan S, von Bergen M, Mandelkow EM, Mandelkow E. Biochemistry. 2008; 47:10526–10539. [PubMed: 18783251]
11. Kim HY, Cho MK, Riedel D, Fernandez CO, Zweckstetter M. Angewandte Chemie. 2008; 47:5046–5048. [PubMed: 18521826]

12. (a) Dias CL, Ala-Nissila T, Wong-ekkabut J, Vattulainen I, Grant M, Karttunen M. Cryobiology. 2010; 60:91–99. [PubMed: 19616532] (b) Ben-Naim A. Journal of biomolecular structure & dynamics. 2012; 30:113–124. [PubMed: 22571437]

13. Brovchenko I, Burri RR, Krukau A, Oleinikova A, Winter R. The Journal of chemical physics. 2008; 129:195101. [PubMed: 19026086]

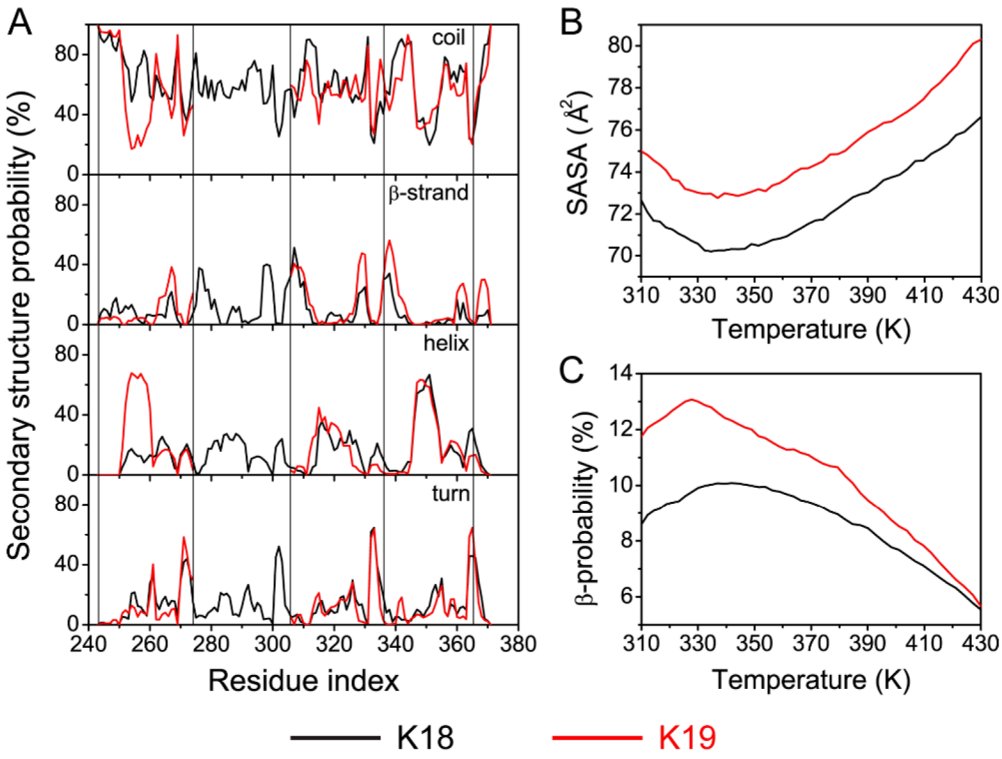

Figure 1.

Tau monomers have temperature-dependent secondary structure propensities and solvent accessibilities. (A) The calculated secondary structure probability of each residue in REMD runs of K18 and K19. Each box corresponds to a repeat. (B) Solvent accessible surface area (SASA) of K18 and K19 at different temperatures indicates that K18 and K19 have the smallest SASA around 335–340 K. (C) K18 and K19 have higher β-strand propensity around 330–350 K.

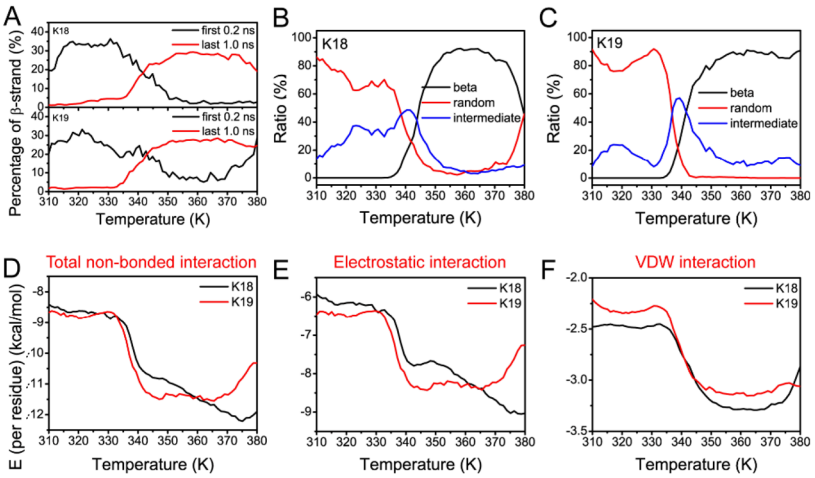

Figure 2.

REMD simulations reveal reversible formation of tau fibrils. (A) The percentage of β-sheet at each temperature within the first 0.2 ns and the last 1.0 ns in the REMD runs. (B)-(C) The ratio of octamer structures versus temperature: conformation with β-sheet propensity less than 5% is defined as random state, conformation with β-sheet propensity higher than 25% is defined as the β-structure, and the others are defined as intermediate states. (D)-(F) Partition of non-bonded interaction energies for tau octamers.

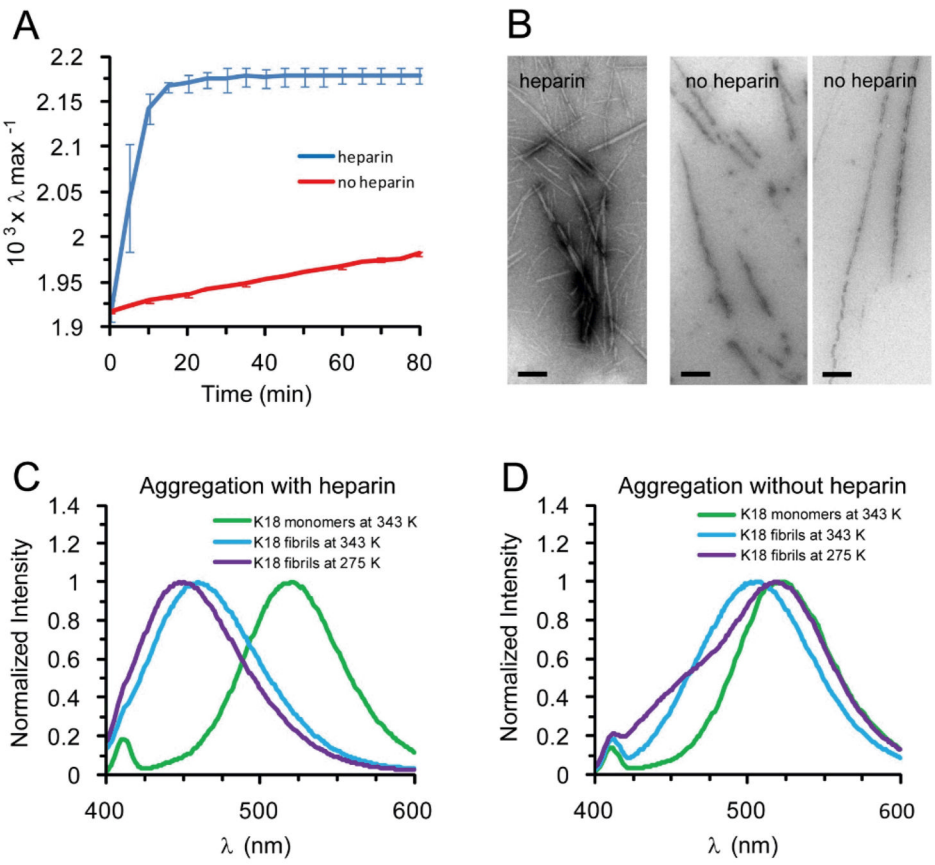

Figure 3.

Heparin locks the tau protein K18 fibril and prevents its reversion. (A) Kinetics of fibril formation at 343 K in the presence (blue) and absence (red) of heparin, as determined by the shift of the emission maximum of acrylodan labeled tau. Values represent mean ±s.d. (n = 3 experiments). (B) EM images of fibrils formed at 343 K in the presence (left panel) and absence (right panels) of heparin. Bar = 200 nm. (C–D) Representative spectra of aggregation reactions in the presence and absence of heparin, respectively. Spectra of monomeric tau (green), after aggregation of fibrils at 343 K (blue), and when cooled to 275 K (purple). Protein concentration = 10 μM. NaCl concentration = 0.1 M. The data indicate that heparin prevents tau fibrils from dissociating in the cold.